CHAPTER V

MAO FREE ETHYLENE POLYMERIZATION WITH IN-SITU ACTIVATED ZIRCONOCENE/TIBA CATALYSTS AND SILICA SUPPORTED STABILIZED BORATE CO-CATALYSTS

5.1 Abstract

Heterogenization of tris(pentafluorophenyl)borane ($B(C_6F_5)_3$) on a silica support stabilized with Chlorotriphenylmethane ($ClCPh_3$) and *N,N*-dimethylaniline ($HNMe_2Ph$) create supported-borane co-catalysts: $[HNMe_2Ph]^+[B(C_6F_5)_3\text{-}SiO_2]^-$ and $[CPh_3]^+[B(C_6F_5)_3\text{-}SiO_2]^-$. These supported catalysts were reacted with Cp_2ZrCl_2/TIBA in-situ to generate active metallocene species in the reactor. Tri-isobutylaluminum (TIBA) was a good co-activator for dichloro-zirconocene, acting as the pre-alkylating substance to generate cationic zirconocene ($Cp_2ZrC_4H_9^+$). The catalytic performances were determined from the kinetics of ethylene consumption profiles that were independent of the time dedicated to the activation of the catalysts. The SEM-EDX measurements show that $B(C_6F_5)_3$, dispersed uniformly on the silica support. Presence of the catalysts on the surface of the support was also seen from XPS measurements. Under our reaction conditions the $[CPh_3]^+[B(C_6F_5)_3\text{-}SiO_2]^-$ system has higher productivity and Mw than the $[HNMe_2Ph]^+[B(C_6F_5)_3\text{-}SiO_2]^-$ system. For $[CPh_3]^+[B(C_6F_5)_3\text{-}SiO_2]^-$ system, the productivity increased with the amount catalyst, however, the PDI of polyethylene synthesized did not change. The final shape of polymer particles was a larger diameter version of the original support particle. The polymer particles synthesized with supported $[CPh_3]^+[B(C_6F_5)_3\text{-}SiO_2]^-$ catalysts had larger diameters.

5.2 Introduction

The polymerization of α-olefins, catalyzed by cationic metallocene of early transition metals, has been studied extensively in recent years [1]. Most of the recent research has been on modification of both the metallocene cation and the associated activators and co-catalysts to enhance productivity and product properties [1a]. One of

the primary requirements for commercial use is that the new catalysts should be useable in the existing polymerization plants without significant plant modification. Replacement of supported Ziegler-Natta catalysts with metallocenes immobilized on inert supports is perhaps the most direct way of introducing new metallocene catalysts into existing plants. This direct replacement is also called "*drop-in technology*". Some of the major advantages of using supported metallocenes over their unsupported counterparts are: reduced need of aluminoxane compounds (e.g. methylaluminoxane, [MAO]), avoiding fouling of the polymerization reactor, production of a good morphology polymer, and high bulk density of the product [3,4].

The most commonly employed supports for metallocene or Ziegler-Natta catalysts are silica (SiO_2), alumina (Al_2O_3), and magnesium chloride ($MgCl_2$) [4]. Other support materials have been investigated but they are not yet commercialized such as zeolites [5], polystyrene [6], etc. The primary means of preparing heterogeneous metallocenes start with the pretreament of a support with alkyl aluminums or MAO followed by the addition of the metallocene [3]. In this preparation the transition metal part of the metallocene remains attached to the support through the same electrostatic forces existing between the metallocene cation and the aluminoxane counterion in solution.

Alternative activators not requiring the presence of MAO for polymerization have been reported. These are Tris(pentafluorophenyl)borane ($B(C_6F_5)_3$), Trityl tetrakis(pentafluorophenyl)-borate ($[CPh_3]^+[B(C_6F_5)_4]^-$), *N,N*-dimethylanilime tetrakis(pentafluorophenyl)-borate ($[HNMe_2Ph]^+[B(C_6F_5)_4]^-$) which create equilibrium concentrations of the catalytically active species $[Cp_2MR]^+$. The activity and stability of these compounds depend on the weakly coordinating character of the counterion species such carbenium ($[CPh_3]^+$) and anilinium ($[HNMe_2Ph]^+$) with $[B(C_6F_5)_4]^-$ [2].

Generally, the surface of oxide supports are covered with Bronsted acidic hydroxyl group (-OH) and Lewis basic oxide groups [7]. Reaction of a simple metallocene with these reactive sites can create Lewis acidic metal centers by losing X group of Cp_2MX_2 (X = CH_3 or Cl) [8]. The mechanisms of supporting a metallocene on Al_2O_3 and $MgCl_2$ were studied with C^{13} CP MAS NMR. The extraction of X

group can result in a cationic-like species which binds to the Lewis acid sites on the support surface [9].

There are many reports of successful preparations of supported organoborane compounds with oxide supports [2b]. These borane-functionalized supports can create very eletrophillic sites on the surface, and form strong Lewis acid sites on the metal species after reacting with metallocenes. Recently these catalysts showed good activity in ethylene polymerization with a low usage of MAO [10].

Hlatky et al. investigated the formation of ionic metallocene generated from metallocene/borate-supported catalysts such as $[Cp_2ZrMe]^+[\ B(C_6F_5)_4\text{-}SiO_2]^-$. These catalyst systems presented very high activity when reacted with dimethyl metallocene catalysts [11]. Bochmann et al.[12] studied the heterogenization of $B(C_6F_5)_3$ activators on silica support by directly impregnating dimethylaniline, $[NMe_2Ph]$ to create $[HNMe_2Ph]^+[B(C_6F_5)_3\text{-}SiO_2]^-$ and then ion exchange with $[CPh_3]^+$ to create $[CPh_3]^+[B(C_6F_5)_3\text{-}SiO_2]^-$. These materials can stabilize the anionic character of functionalized borane-oxide on silica surface ($OB(C_6F_5)_3^-$). The cationic species can bind the anionic borate by ionic-bonding rather than covalent interactions. Bochmann et al's results showed good catalytic activity for ethylene polymerization after reacting with dimethyl zirconocene [12]. In addition Ward et al. [13] developed a different kind of supported-borane catalysts (e.g. $[CPh_3]^+[B(C_6F_5)_3\text{-}SiO_2]^-$) by providing a catalyst activator which had lithilated hydroxyl groups on silica support after reacting the support with BuLi. After litilation of the hydroxyl groups $B(C_6F_5)_3$ is chemically bound to the support, which is followed by addition of $ClCPh_3$. This preparation reduced the resolubilization of $B(C_6F_5)_3$ from the surface of heterogeneous catalysts, and minimized the fouling affect in polymerization processes. However most of the previous research required a dialkyl metallocene to generate the weakly coordinating metallocenium salts.

Recently, novel in-situ activated catalyst systems showed remarkable kinetic profiles for ethylene polymerization. Their activities did not rapidly decay and showed time independent ethylene consumption when zirconocene was reacted directly with supported MAO inside the reactor [14]. Therefore the kinetic profiles are very important in providing information about the active species and catalysis decay status in polymerization processes [14,15].

In this work we report the preparation and characterizations of anilinium and carbenium supported-borane co-catalysts on silica for making "aluminoxane-free" supported catalysts. We also studied the kinetic profiles of ethylene polymerization for different supported-borane activators with in-situ activation.

5.3 Experimental

5.3.1 Materials

Polymerization grade ethylene and UHP grade nitrogen (Cryogenic, Michigan) were dried by passing through a column of oxygen-moisture trap (MATHESON). Tris(pentafluorophenyl)borane ($B(C_6F_5)_3$) solution (11%wt in toluene), Trityl tetrakis(pentafluorophenyl)borate ($[CPh_3]^+[B(C_6F_5)_4]^-$), *N,N*-dimethylaniline tetrakis(pentafluorophenyl)borate ($[HNMe_2Ph]^+[B(C_6F_5)_4]^-$) were obtained from Albemarle. Silica gel (Sylapol^{TM} 948 donated by W.R. Grace company, Maryland) had a surface area of 309 m^2/g, and pore volume of 1.62 cc/g. Bis(cyclopentadiene)zirconiumdichloride (Cp_2ZrCl_2), triisobutylaluminum (TIBA, solution 1.0 M in toluene), Chlorotriphenylmethane ($ClCPh_3$), and *N,N*-dimethylaniline (NMe_2Ph) were purchased from Aldrich. Toluene (Aldrich, anhydrous grade, $H_2O < 0.001\%$) was purified by refluxing with sodium for 48 h, then degassed by distillation under N_2 with CaH_2 reflux, and stored over 3A molecular sieves before use. Hexane was out gassed by bubbling with N_2 and stored over 3A molecular sieves before use.

5.3.2 Catalyst preparation

All of the catalyst preparation steps were carried out under anhydrous and anaerobic conditions in a glove box (O_2 and $H_2O < 1$ ppm).

5.3.2.1 Support treatment

To prepare the partially hydroxylated silica, silica gel support was washed with DI-water and dried at 50 °C under vacuum. Then, it was packed into a horizontal quartz tube and calcined at 500 °C under flowing oxygen. After 6 hours, the temperature was decreased to 25°C with oxygen flow and the silica powder was stored under vacuum until use.

5.3.2.2 The preparation of $[HNMe_2Ph]^+[B(C_6F_5)_3\text{-}SiO_2]^-$ catalyst

The treated silica gel (~ 2 g) and toluene (14 ml) were mixed as slurry in a volumetric flask (100 ml) equipped with a magnetic stirrer bar. $B(C_6F_5)_3$ (1.26 mmol in 6 ml of toluene) and NMe_2Ph (1.26 mmol) were pre-mixed and added dropwise to the stirred slurry of silica gel. After stirring the mixture for 12 h at room temperature, the slurry was left to settle overnight. The solid part was collected with a medium fritted flask. The product was washed with toluene (3x5 ml) and hexane (2x5 ml) and then dried in vacuum for 4 h to yield 2.12 g of white solid (some mass was lost during transfer).

5.3.2.3 The preparation of $[CPh_3]^+[B(C_6F_5)_3\text{-}SiO_2]^-$ catalyst

The treated silica gel (~ 2 g) and toluene (14 ml) were mixed as slurry in a volumetric flask (100 ml) equipped with a magnetic stirrer bar and then mixed with $B(C_6F_5)_3$ (1.26 mmol in 6 ml of toluene). The slurry mixture was stirred for 3 h. $ClCPh_3$ (1.26 mmol or 0.351 g) in toluene (4 ml) was added dropwise to the mixture in the dark. After stirring the mixture for 12 h at room temperature, the slurry was left to settle overnight. The solid part was collected with a medium fritted flask. The filtered solid was washed with toluene (4x10 ml) and hexane (4x10 ml) and then dried in vacuum for 4 h to yield 2.38 g of yellowish solid (some mass was lost during transfer).

5.3.3 Polymerization system and procedures

The ethylene polymerization was carried out in a 500 ml stainless steel reactor (Pressure Product Industrial) equipped with a dynamic magnetic stirrer and a Teflon liner. The polymerization temperature was controlled using a PID temperature controller (OMEGA, CN-8502) with a heating jacket and a cooling U-coil (water as coolant) inside the reactor. The temperature was measured using a thermocouple (OMEGA, K-type) immersed in a thermowell. The rate of ethylene consumption was monitored by using a mass-flow-meter (Cole-Parmer, model no. 32915-14) linked to a computer (LAB-VIEW v5.5 software) used to acquire the temperature and flow rate data as a function of time.

Prior to each run, the reactor was dried at 150 ^{0}C under vacuum for one hour. The reactor was cooled down while flushing with pure nitrogen for several times and ethylene for the last cycle. The stirring speed was kept constant at 1000 rpm. All chemicals made as solutions in toluene were loaded into a cylindrical bomb under an inert atmosphere to transfer into the reactor by N_2 overpressure. First, 200 ml of toluene was introduced into the reactor and the temperature was set to 40°C. For the homogeneous system, a desired amount of zirconocene and TIBA were loaded into the reactor and the reactor was pressurized with ethylene at 20 psig. After 5 min, a weighted amount of the co-catalyst, was loaded into the reactor to start the polymerization. For the heterogeneous system, the prescribed amounts of zirconocene and TIBA were loaded into the reactor that was pressurized with ethylene at 20 psig. After 5 min, a weighted amount of the co-catalyst, suspended in 10 ml of toluene, was loaded into the reactor. The temperature was controlled to ±1 ^{o}C of the set point. After 30 min, the reactor was cooled to room temperature and depressurized. 10 ml of acidic-methanol was injected into the reactor to quench the system. The final product was washed with an excess of methanol a few times, filtered, and left in the hood for 4 days.

5.3.4 Catalyst characterizations

The bulk concentration of boron (in $B(C_6F_5)_3$) on the silica support was determined by using an Inductively Coupled Plasma Atomic Emission Spectrometer (ICP-AES Leeman Labs Plasma-Spec ICP Model 2.5). Samples for testing were prepared by digesting the catalyst powder in a 4 N aqueous solution of HNO_3. A calibration curve was run prior to the samples and an independent check was run interspersed with the samples.

X-ray Photoelectron Spectroscopy (XPS, Perkin Elmer PHI 5400 model) was used to identify surface species as well determining the binding energy of electrons in the catalyst. The spectra were scanned at room temperature in with a resolution of 0.1 eV in the range of 0-800 eV. Samples were pressed to form a pellet under an inert gas and then placed on the sample holder. The spectra of B (1s) at 191 eV and F (1s) at 690 eV were determined at 90^{o} angle relative to the electron detector.

The morphology of the supported catalysts was determined by Scanning Electron Microscopy (SEM, Philips XL30 SEM). Due to the low electron emission samples, the sample must be sputtered and coated with carbon prior to test. Fluorine (F-K) distribution was provided by using the Energy Dispersed X-ray detector equipped with SEM and EDX control software.

5.3.5 Polymer characterization

The average molecular weights (Mw) and molecular weight distributions (MWD) or polydispersity indices (PDI) of the polyethylene products were determined using a high-temperature gel permeation chromatograph (GPC) equipped with three Waters Ultrastyragel columns in series at 150 ^{o}C with o-dichlorobezene as solvent. The columns were calibrated with narrow molecular weight distribution polystyrene samples. The morphology of the polymers was investigated using scanning electron microscopy (SEM, Philips XL30 SEM). The bulk density of the polymer particles was measured according to ASTM Standard D 1895.

5.4 Results and Discussion

5.4.1 Catalyst characterization

The natural silica surface is covered with silanol groups, at a maximum concentration of 8 Bronsted acidic OH groups per square nm. These silanol groups are mostly composed of geminal and isolated pairs and have neither very acidic nor very basic characters [9]. The hydroxylated surface is hydrophilic and easily adsorbs moisture from the air. Adsorbed water can have elimination, esterification or condensation reactions with the silanol groups and is normally presents in sufficient quantities to change almost all Lewis sites into Bronsted sites. After heat treatment at 500 °C, this physically adsorbed water can be removed and a partially hydroxylated silica gel surface is left behind. The absolute number of the hydroxyl groups may differ from sample to sample according to the methods of preparation which may yield different ratios of various crystal planes on the surface [16].

After refluxing the treated silica in an excess of $B(C_6F_5)_3$, and either anilinium or carbenium salts, the coordination complexes between $B(C_6F_5)_3$ and the oxygen atom of the hydroxyl groups can change into anionic active species stabilized by the cationic salts. The previous FT-IR result have shown that not all OH groups of silica are accessible to coordinate with $B(C_6F_5)_3$ [12b]. As shown in Table 5.1, in the presence of cationic salts almost 100 % of the borane in solution is adsorbed onto the support surface.

The amount of $B(C_6F_5)_3$, was determined by using ICP-AES Only attached $B(C_6F_5)_3$ on silica support was detected by ICP-AES and the error from ICP-AES measurements was estimated to be around 15% in all of the experiments. We found that different solvents used in the washing step had different efficiencies to remove the unbound $B(C_6F_5)_3$ from the pores of the support. With a solvent such as hexane the structure of the synthesized polyethylene resembled the product from homogeneous systems. Therefore the choice of the solvent in the preparation was important to maintain the heterogeneous character of the co-catalyst. Figure 5.1 shows a proposed mechanism of funtionalization of borane on the silica support.

The surface concentration of all elements on the silica surface was investigated by XPS. As the XPS analysis is limited to the sample on the surface, the results from XPS cannot be directly compared with the bulk technique. Figure 5.2 shows the survey XPS spectra for $[HNMe_2Ph]^+[B(C_6F_5)_3\text{-}SiO_2]^-$ and $[CPh_3]^+[B(C_6F_5)_3\text{-}SiO_2]^-$ catalysts and calcined pristine silica. The presence of the elements F, O, C, B, Si, were measured with XPS to a sampling depth of about 3 μm. The presence of boron and fluorine peaks in the survey spectra show that $B(C_6F_5)_3$ was grafted on the silica surface.

The scanning electron micrograph (SEM) in Figure 5.3a shows the typical catalyst particle after the preparation steps. The morphology of the $[HNMe_2Ph]^+[B(C_6F_5)_3\text{-}SiO_2]^-$ catalyst is spherical. The distribution of active $B(C_6F_5)_3$ species on the silica surface was observed by using SEM with energy dispersive X-ray detector (EDX). As shown in figure 5.3b, the Fluorine containing molecules are uniformly dispersed on the support surface.

5.4.2 Catalytic activity in ethylene polymerization

In all the experiments zirconocene dichloride (Cp_2ZrCl_2) was pre-alkylated with TIBA before adding the supported borane co-catalysts. This reaction is believed to be fast and gives as the final species cationic zirconocene (Cp_2ZrBu^+) [17-19]. In general during our polymerization studies, we had no reproducibility problems with respect to the ethylene consumption profiles, productivities or molecular weights and the morphology of the polymer independent on the catalyst system used.

The results of ethylene polymerization with $[HNMe_2Ph]^+[B(C_6F_5)_3\text{-}SiO_2]^-$ and $[CPh_3]^+[B(C_6F_5)_3\text{-}SiO_2]^-$ co-catalysts and Cp_2ZrCl_2/TIBA are shown in Table 5.2. Under the same reaction conditions $[CPh_3]^+[B(C_6F_5)_3\text{-}SiO_2]^-$ co-catalyst gives higher activities as well as higher molecular weight. Increasing the amount of the $[CPh_3]^+[B(C_6F_5)_3\text{-}SiO_2]^-$ catalyst increased the activity for ethylene polymerization as well as the average molecular weight. However, there were no detectable differences in the polydispersities. Moreover the ethylene consumption profile did not change significantly with the catalyst amount and continued to show

no loss of activity with time as shown in figure 5.4. We also observed a solvent effect. The co-catalyst that was washed only with hexane had high productivity but produced polyethylene with poor morphology. We believe this is due the extraction of $B(C_6F_5)_3$ into the toluene solvent during the polymerization. Even though we were using $[CPh_3]^+[B(C_6F_5)_3\text{-}SiO_2]^-$ co-catalyst, the Mw of polyethylene synthesized from it was not significantly different from the homogeneous analog when the amount of supported co-catalyst used was below 0.2 g. In comparison the homogeneous borate co-catalyst systems of Cp_2ZrCl_2/TIBA/$[CPh_3]^+[B(C_6F_5)_4]^-$, and Cp_2ZrCl_2/TIBA/$[HNMe_2Ph]^+[B(C_6F_5)_4]^-$ (Runs 10 and 11) gave very low productivities of polyethylene for 1:1 of the Zr:B ratio. We suspect this may be because of formation of isolable binuclear compounds or in the presence of TIBA, cationic active metallocenes may transform to deactivated forms [20,21]. Also their ionic characters limit solubility, particularly in saturated hydrocarbons, as well as long-term stability in storage.

We also carried out ethylene polymerization with the $[HNMe_2Ph]^+[B(C_6F_5)_3\text{-}SiO_2]^-$ co-catalysts (Figure 5.5). Again the ethylene polymerization was conducted with the Cp_2ZrCl_2/TIBA using the in situ activation of the catalyst. This system showed some decay in its ethylene consumption profile. The time independence observed with the carbenium salts is most likely due to regeneration of active metallocene sites during polymerization [2,14].

SEM pictures of the polymer products of both co-catalyst systems were taken to observe their morphology. The SEM pictures in Figure 5.6, clearly show the dramatic difference in the shape of the polymer particle synthesized by the homogeneous system and the one synthesized by the $[HNMe_2Ph]^+[B(C_6F_5)_3\text{-}SiO_2]^-$ and $[CPh_3]^+[B(C_6F_5)_3\text{-}SiO_2]^-$ co-catalyst systems. Similar to the morphology of polymer produced from heterogeneous Ziegler-Natta catalysts, the final shape of polymer particle produced by the heterogeneous metallocene catalyst system is a mimicked spherical particle of the original catalyst support and has free-flowing character in any solvents [5]. The diameters of the polymer particles are larger than the original support particle by about 10 times. Under the same reaction conditions, the polymer produced from $[CPh_3]^+[B(C_6F_5)_3\text{-}SiO_2]^-$ system had larger particles than that produced from $[HNMe_2Ph]^+[B(C_6F_5)_3\text{-}SiO_2]^-$ system. The polymer produced by the

homogenous system displayed irregular structure and has "sponge-like" morphology, which results in a lower bulk density. As can be seen in table 5.2 the bulk densities of the polymer particles produced by the supported catalysts are at least five times higher than the bulk density of the polymer from the homogeneous system. Furthermore the bulk density of the polymer produced by the $[CPh_3]^+[B(C_6F_5)_3\text{-}SiO_2]^-$ co-catalyst system are somewhat higher than the bulk densities of the polymers from the $[HNMe_2Ph]^+[B(C_6F_5)_3\text{-}SiO_2]^-$ co-catalyst system. The bulk density also seems to increase for both co-catalyst systems with increasing catalyst concentration.

Although both catalysts produced spherical polymer particles, the experimental parameters and the length of the polymerization period were important to control final morphology of the polymer particle. The polymer particles of the $[HNMe_2Ph]^+[B(C_6F_5)_3\text{-}SiO_2]^-$ co-catalyst system have a more nonuniform and open surface whereas the $[CPh_3]^+[B(C_6F_5)_3\text{-}SiO_2]^-$ co-catalyst system polymer particles have a much more uniform surface as seen by comparing figures 5.6b (Run 3) and 5.6c (Run 9). Under the polymerization conditions, the spherical polymer particles may have non-uniform surface morphology because of the localization of catalytically active sites on the support surface during the polymerization.

In addition, the regularity of the surface of polymer particle depends on the distribution of active species on the surface support. In general the active borane on silica support was difficultly reached with active metallocene after the initial period of the polymerization, the surface of where has higher concentration of borane can be more accessibly than of where has lower concentration of borane. Another reason may be from external factors such as the polymerization temperature; which may lead to mass transfer limitations during the growth of the polymer particle.

5.5 Conclusions

We have succeeded in preparing supported-borane co-catalysts by grafting $B(C_6F_5)_3$ onto Bronstead acid sites on silica surface and stabilized it with $[HNMe_2Ph]^+$ and $[CPh_3]^+$ salts. The resulting catalysts had uniformity distributed catalytic sites throughout the support, rather than being isolated on the surface alone.

The heterogenous metallocene catalysts prepared in this study showed high activity for ethylene polymerization after in-situ activation of the metallocene with TIBA without the need for aluminoxane compounds. The activity of the catalysts was constant with respect to time up to thirty minutes (the maximum that our reactor could handle). The $[CPh_3]^+[B(C_6F_5)_3\text{-}SiO_2]^-$ co-catalyst showed especially high activities and high molecular weights and high bulk densities. The polymer particles had excellent morphology with spherical shapes and uniform surfaces.

5.6 References

1. For recent reviews, see: (a) Gladysz, J. A. Chem Rev 2000, 100, 1167-1168. (b) Hlatky, G.G. Coord Chem Rev 1999, 181, 243-296. (c) Hlatky, G.G. Coord Chem Rev 2000, 199, 235-329. (d) Britovsek, G. J. P.; Gibson, V. C.; Wass, D. F. Angew Chem, Int Ed Engl 1999, 38, 428-447. (e) Brintzinger, H. H.; Fischer, D.; Mülhaupt, R.; Rieger, B.; Waymouth, R. M. Angew Chem, Int Ed Engl 1995, 34, 1143-1170.
2. (a) Bochmann, M. Top Catal 1999, 7, 9-22. (b) Chen, E. Y.X.; Marks, T. J. Chem Rev 2000, 100, 1391-1434.
3. (a) Ribeiro, M. R.; Deffieux, A.; Portela, M. F. Ind Eng Chem Res 1997, 36, 1224-1237. (b) Chien, J. C.W. Top Catal 1999, 7, 23-36.
4. Muñoz-Escalona, A.; Mémdez, L.; Sancho, J.; Lafuente, P.; Peña, B.; Michiels, W.; Hidalgo, G.; Martínez-Nuñez, M. F. Metalorganic Catalysts for Synthesis and Polymerization; Kaminsky, W. Eds.; Springer-Verlag: Berlin, 1999, pp 381-396.
5. Ciardelli, F.; Altomare, A.; Michelotti, M.; Arribas, G.; Bronco, S. Metalorganic Catalysts for Synthesis and Polymerization; Kaminsky, W. Eds.; Springer -Verlag: Berlin, 1999, pp 358-367.
6. (a) Klapper, M.; Koch, M.; Stork, M.; Nenov, N.; Műllen, K. Organometallic Catalysts and Olefin Polymerization; Blom, R.; Follestad, A.; Rytter, E.; Tilset, M.; Ystenes, M. Eds.; Springer-Verlag: Berlin, 2001, pp 387-395. (b) Roscoe, S. B.; Fréchet, J. M. J.; Walzer, J. F.; Dias, A. J. Science 1998, 280,

270-273. (c) Kishi, N.; Ahn, C. H.; Jin, J.; Uozumi, T.; Sano, T.; Soga, K. Polymer 2000, 41, 4005-4012.

7. Fink, G.; Steinmetz, B.; Zechlin, J.; Przybyla, C.; Tesche, B. Chem Rev 2000, 100, 1377-1390.
8. Marks, T. J. Acc. Chem Res 1992, 25, 57-65 and references therein.
9. (a) Finch, W. C.; Gillespie, R. D.; Hedden, D.; Marks, T. J. J. Am. Chem. Soc. 1990, 112, 6221-6232. (b) He, M. Y.; Burwell, R. L. Jr.; Marks, T. J. Organometallics 1983, 2, 566-569. (c) Dahmen, K. H.; Hedden, D.; Burwell, R. L. Jr.; Marks, T. J. Langmuir 1988, 4, 1212-1214.
10. Tian, J.; Wang, S.; Feng, Y.; Li, J.; Collins, S. J Mol Catal A 1999, 144, 137-150.
11. (a) Hlatky, G. G.; Upton, D. J. Macromolecules 1996, 29, 8019-8020. (b) Hlatky, G. G.; Upton, D. J.; Turner, H. W. Europe Patent, EP-507876B1, 1995.
12. (a) Bochmann, M.; Jiménez Pindado, G.; Lancaster, S. J. J Mol Catal A 1999, 146, 179-190. (b) Lancaster, S. J.; O'Hara, S. M.; Bochmann, M. Metalorganic Catalysts for Synthesis and Polymerization; Kaminsky, W. Eds.; Springer-Verlag: Berlin, 1999, 413-425.
13. Ward, D. G.: Carnahan, E. M. U.S. Patent 5,939,347, 1999 (W. R. Grace).
14. (a) Chu, K. J.; Soares, J. B. P.; Penlidis, A. J Polym Sci, Polym Chem 2000, 38, 462-468. (b) Chu, K. J.; Soares, J. B. P.; Penlidis, A. Macromol Chem Phys 2000, 201, 552-557.
15. Naga, N.; Shiono, T.; Ikeda, T. J Mol Catal A 1999, 150, 155-162.
16. Jezequel, M.; Dufaud, V.; Ruiz-Garcia, M. J.; Carrillo-Hermonsilla, F.; Neugebauer, U.; Niccolai, G. P.; Lefebvre, F.; Bayard, F.; Corker, J.; Fiddy, S.; Evans, J.; Broyer, J. P.; Malinge, J.; Basset, J. M. J Am Chem Soc 2001, 123, 3520-3540.
17. Haselwander, T.; Beck, S.; Brintzinger, H. H. Ziegler Catalysts; Fink, G.; Mülhaupt, R.; Brintzinger, H. H. Eds.; Springer-Verlag: Berlin, 1995, pp 181-197.
18. Beck, S.; Prosenc, M. H.; Brintzinger, H. H. J Mol Catal A 1998, 128, 41-52.

19. (a) Chien, J. C.W.; Song, W.; Rausch, M. D. Macromolecules 1993, 26, 3239-3240. (b) Chien, J. C.W.; Tsai, W. M.; Rausch, M. D. J Am Chem Soc 1991, 113, 8570-8571. (c) Chien, J. C.W.; Song, W.; Rausch, M. D. J Polymer Sci A 1994, 32, 2387-2393.

20. Bochmann, M.; Lancaster, S. J. Angew Chem Int Ed Engl 1994, 33, 1634-1637.

21. Zhou, J.; Lancaster, S. J.; Walker, D. A.; Beck, S.; Thornton-Pett, M.; Bochmann, M. J Am Chem Soc 2001, 123, 223-237.

Table 5.1 The adsorption of borane on silica support.

Supported co-catalysts	B (mmol/g) [1]	% Borane in the original solution adsorbed on silica[2]
$B(C_6F_5)_3$-SiO_2	0.22	35 %
$[HNMe_2Ph]^+[B(C_6F_5)_3$-$SiO_2]^-$	0.60	90 %
$[CPh_3]^+[B(C_6F_5)_3$-$SiO_2]^-$	0.64	~ 100 %
$B(C_6F_5)_3$ (standard)[3]	3.64[4]	-

[1] from ICP-AES analysis

[2] Calculated from the original amount of $B(C_6F_5)_3$ in solution

[3] Standard solution of $B(C_6F_5)_3$ ~ 3.614 mmol

[4] Unit is mmol

Table 5.2 Catalytic activity of supported borate catalysts.

Run	Type of supported catalyst[1]	[Zr] (μmol)[2]	Support (g)	Productivity[3]	Mw (x 10^{-4})	PDI	Bulk density (g/mL)
1	BN	38.7[4]	0.38	0.17	9.8	10.3	-
2	BN	2	0.22	1.22	7.8	3.8	0.18
3	BN	4	0.24	1.68	9.3	4.2	0.24
4	BN	12.9	0.28	2.85[5]	9.4	16.2	-
5	BC	2	0.14	1.24	7.4	3.0	-
6	BC	2	0.20	1.43	9.7	3.1	0.19
7	BC	2	0.30	4.41	12.4	3.1	0.28
8	BC	2	0.40	5.40	38.8	3.1	0.35
9	BC	4	0.20	3.17	38.2	4.4	-
10[6]	BrC	2	-	1.12	8.3	2.2	0.05
11[6]	BrN	2	-	0.12	4.3	2.1	0.05

Polymerization conditions: TIBA = 1 mmol, toluene = 240 ml, Tp = 40 °C, Ethylene = 20 psig, Time = 30 min, Zr = Cp_2ZrCl_2

[1]BN=$[HNMe_2Ph]^+[B(C_6F_5)_3\text{-}SiO_2]^-$, BC= $[CPh_3]^+[B(C_6F_5)_3\text{-}SiO_2]^-$,
BrC= $[CPh_3]^+[B(C_6F_5)_4]^-$, BrN= $[HNMe_2Ph]^+[B(C_6F_5)_4]^-$

[2]Zr = Cp_2ZrCl_2

[3] productivity = kgPE/mmol of Zr · atm · h

[4]Al = 2 mmol

[5] The supported catalyst was washed only by hexane after loading the borane, product is identical with PE obtained with the homogenous zirconocene system.

[6]Homogeneous with B:Zr = 1

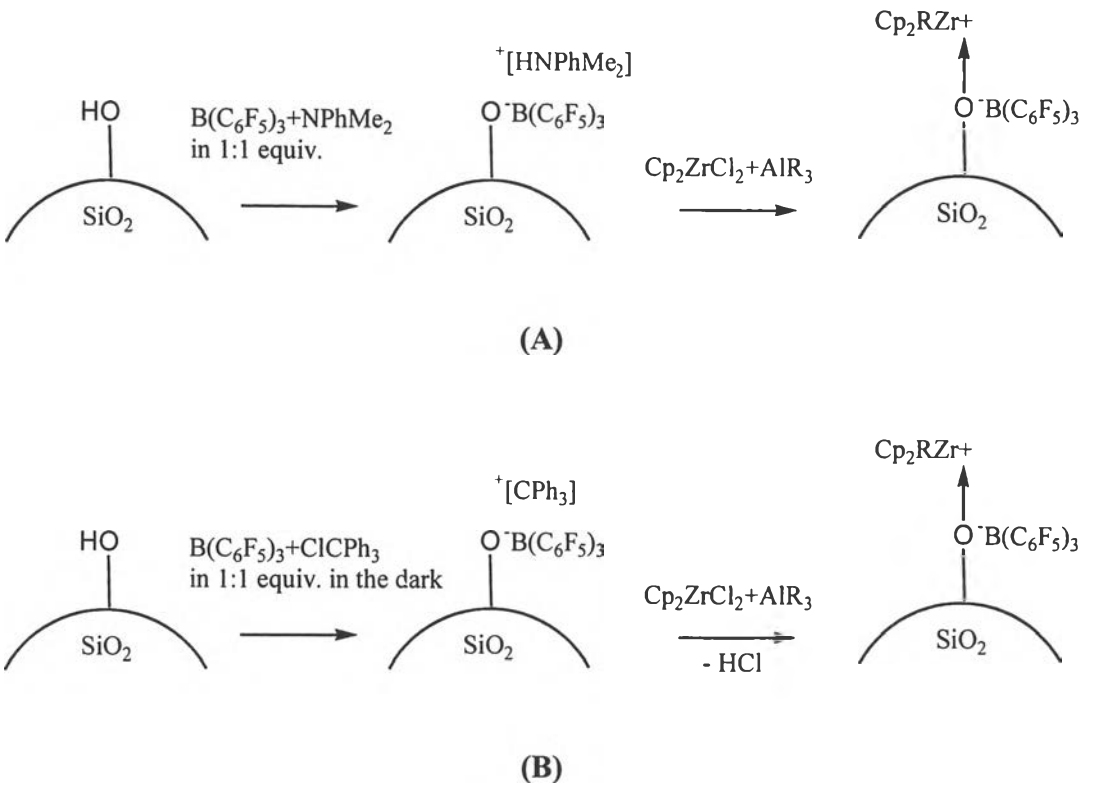

Figure 5.1 The mechanisms of borate-supported activating metallocene: (A) $[HNMe_2Ph]^+[B(C_6F_5)_3\text{-}SiO_2]^-$,(B) $[CPh_3]^+[B(C_6F_5)_3\text{-}SiO_2]^-$.

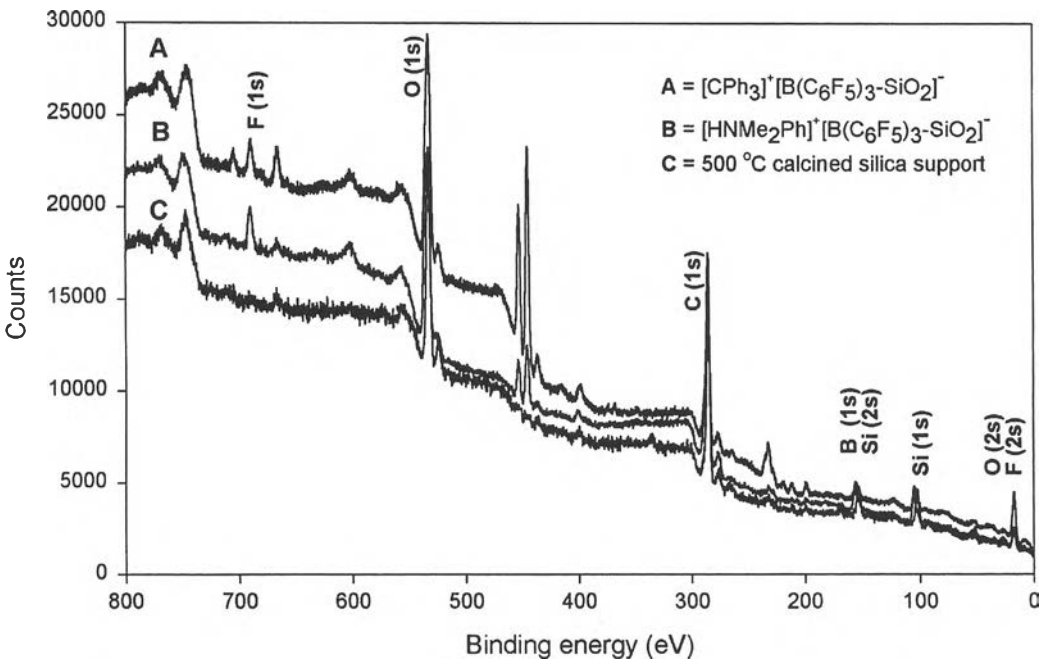

Figure 5.2 XPS survey spectra of silica supported borate catalysts to show the elements detected on the silica surface.

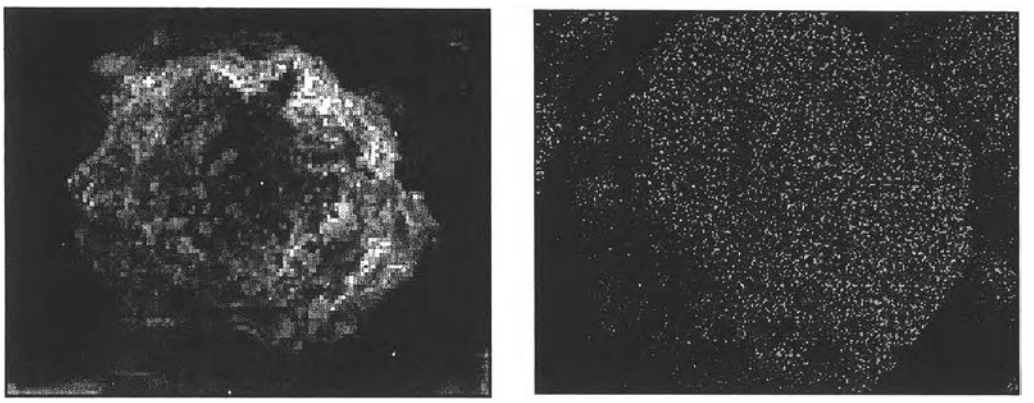

(A) **(B)**

Figure 5.3 (A) SEM picture of $[HNMe_2Ph]^+[B(C_6F_5)_3\text{-}SiO_2]^-$ catalyst, (B) Fluorine mapping (F-K) of $B(C_6F_5)_3$ on silica support. The uniformity of the distribution of the fluorine atoms on the surface is evidence that the support is uniformly loaded with the borane co-catalyst.

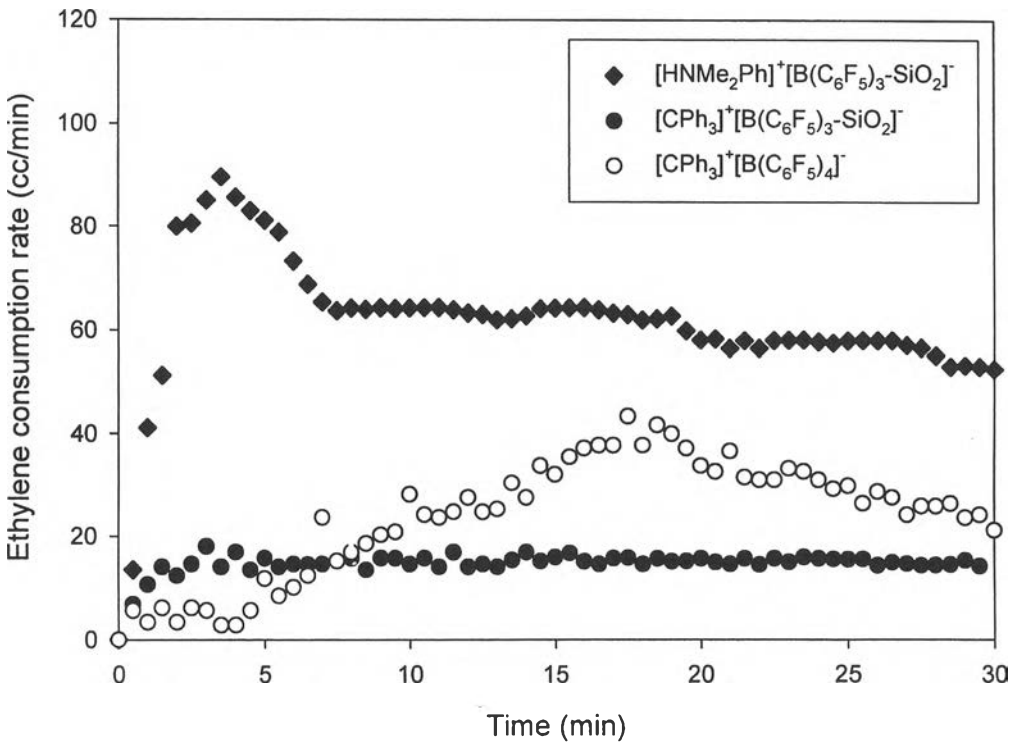

Figure 5.4 Kinetic profiles of ethylene polymerization with various supported catalysts: $[HNMe_2Ph]^+[B(C_6F_5)_3\text{-}SiO_2]^-$ from Run 3, $[CPh_3]^+[B(C_6F_5)_3\text{-}SiO_2]^-$ from Run 6, and $[CPh_3]^+[B(C_6F_5)_4]^-$ from Run 10.

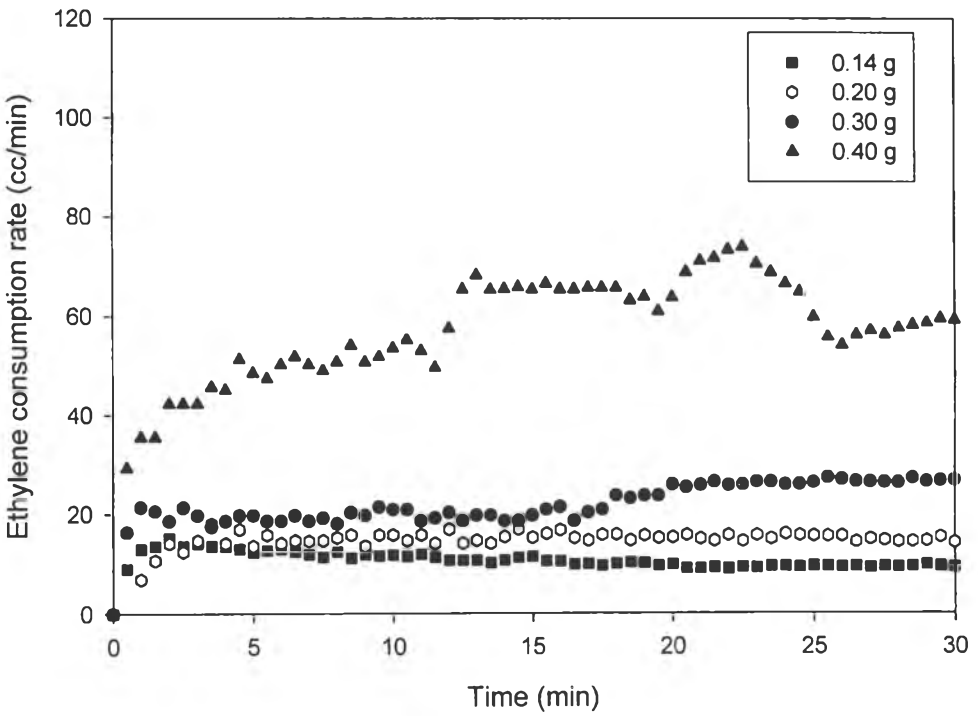

Figure 5.5 Effect of amount of $[CPh_3]^+[B(C_6F_5)_3\text{-}SiO_2]^-$ on kinetic profiles of ethylene polymerization: [Zr] = 2 μmol, Al:Zr = 400, T_p = 40 °C, Ethylene = 20 psig.

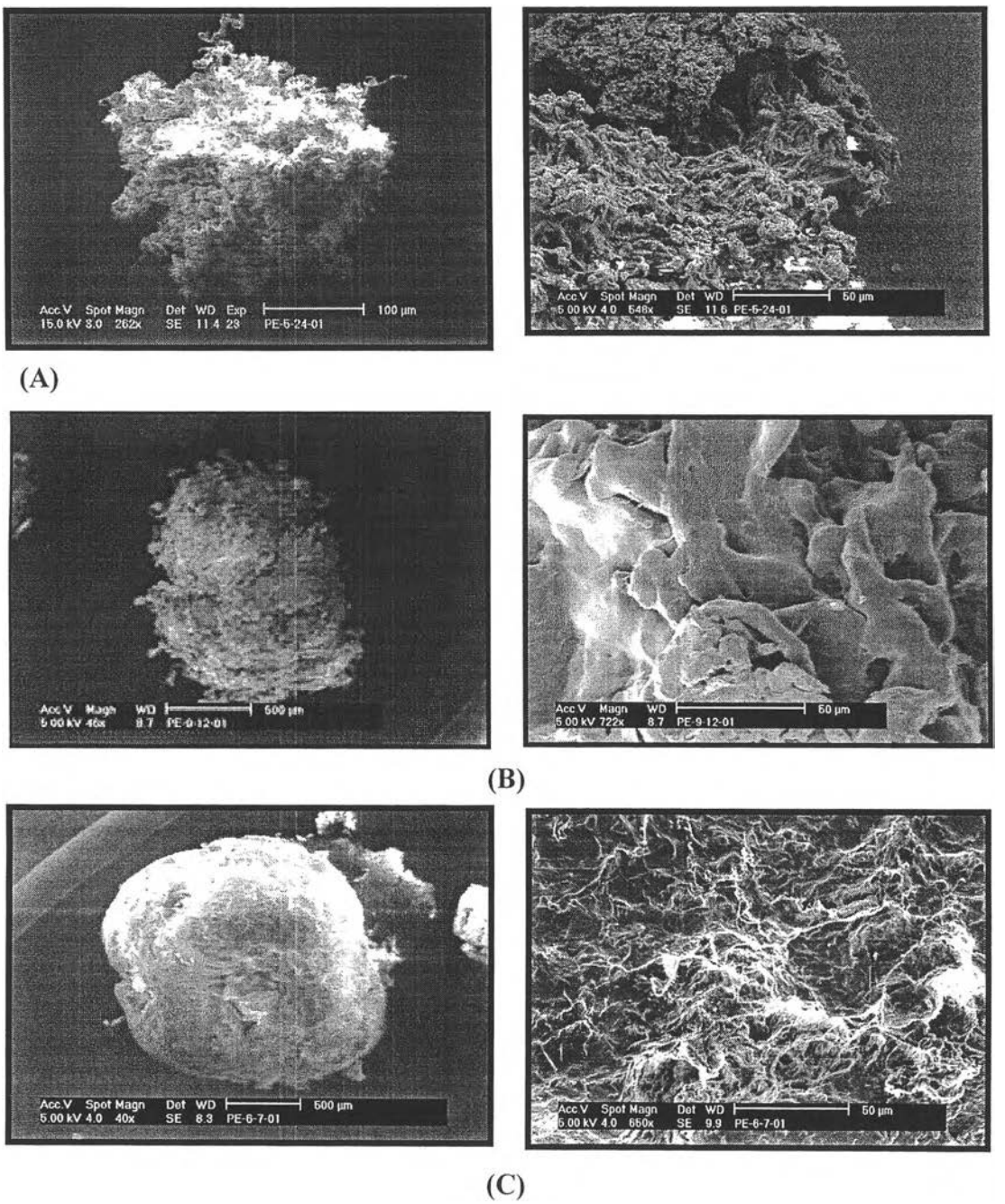

Figure 5.6 SEM micrographs of polyethylene grains: **(A)** from $[CPh_3]^+$ $[B(C_6F_5)_4]^-$ system (Run 10) **(B)** from $[HNMe_2Ph]^+[B(C_6F_5)_3\text{-}SiO_2]^-$ system (Run 3), **(C)** from $[CPh_3]^+[B(C_6F_5)_3\text{-}SiO_2]^-$ system (Run 9).